NASA TECHNICAL NOTE

NASA TN D-3108

c. 1

NASA TN D-3108

AN INVESTIGATION OF THE INTENSITIES AND CHARGE COMPOSITION OF LOW ENERGY ELECTRONS AT BALLOON ALTITUDES

by Peter Serlemitsos

Goddard Space Flight Center
Greenbelt, Md.

NATIONAL AERONAUTICS AND SPACE ADMINISTRATION - WASHINGTON, D. C. - DECEMBER 1965

NASA TN D-3108

AN INVESTIGATION OF THE INTENSITIES AND CHARGE COMPOSITION OF LOW ENERGY ELECTRONS AT BALLOON ALTITUDES

By Peter Serlemitsos

Goddard Space Flight Center
Greenbelt, Md.

NATIONAL AERONAUTICS AND SPACE ADMINISTRATION

For sale by the Clearinghouse for Federal Scientific and Technical Information
Springfield, Virginia 22151 – Price $1.00

AN INVESTIGATION OF THE INTENSITIES AND CHARGE COMPOSITION OF LOW ENERGY ELECTRONS AT BALLOON ALTITUDES

by
Peter Serlemitsos
Goddard Space Flight Center

SUMMARY

A detector has been designed and constructed for the purpose of measuring the positron-to-electron ratio at balloon altitudes as a function of electron energy, in the range from about 1 to 15 Mev. The principle of operation as well as problems encountered in design, construction and calibration are discussed. In addition, data from a recent flight over Northern Canada are presented and their implications with regard to the detector's purpose are considered. Possible ways for improving the present apparatus are mentioned along with the apparent limitations of this type of detector when used to conduct cosmic ray research at balloon altitudes.

CONTENTS

AN INVESTIGATION OF THE INTENSITIES AND CHARGE COMPOSITION OF LOW ENERGY ELECTRONS AT BALLOON ALTITUDES*

by
Peter Serlemitsos
Goddard Space Flight Center

INTRODUCTION

The existence of relativistic electrons in detectable quantities, at all altitudes attainable in balloon flight, is well known. These electrons are produced for the most part in cascade showers originating from nuclear interactions of energetic cosmic rays at the top of the atmosphere. In accordance with shower theory and previous experimental results, the number of electrons with energies above a given energy increases with atmospheric depth, reaching a maximum at a depth which depends on the energy threshold. Thus for electrons above about 10 Mev, the maximum particle intensity occurs somewhere between 100 and 200 gm/cm^2 of air. Near the top of the atmosphere, as for example at the typical balloon floating depth of 3 to 4 gm/cm^2, we would expect only a small number of shower products, because of the small probability that a nuclear interaction and a number of radiative processes will occur in succession within such a small fraction of one radiation length of matter. Nevertheless, relatively large electron fluxes have been observed at the depth in question. Transition plots show that the integral electron intensity above a few Mev does not extrapolate at high latitudes to near a zero intensity at the top of the atmosphere (Reference 1), as might be expected if the sole contribution to this component of radiation came from cascade showers.

These electrons must therefore represent one or both of the following: (1) A return albedo, that is, secondaries from the opposite hemisphere which were guided along lines of force of the earth's field; (2) A component of the primary cosmic radiation of solar or galactic origin. There is considerable interest in both of these electron sources. Return albedo measurements are needed as little is known about this particle source. Of far greater importance will be any information obtained concerning the electronic component of solar and/or galactic cosmic rays. It has long been established (Reference 2) that electrons do not comprise more than about 0.6 percent of the primary galactic cosmic ray flux for energies greater than 10^9 ev. Recent observations have produced detectable electron intensities in the energy region around 100 Mev (References 1 and 3).

The galactic electronic component may originate from either or both of the following sources. In the first place, it may have the same origin as the other galactic cosmic radiation. Radio

*Submitted in partial fulfillment of the requirements for a Master of Science degree, University of Maryland, 1963.

astronomy has produced strong evidence that at outbursts of supernovae, large numbers of electrons are created in the expanding envelopes; and thus some of them must surely find their way into interstellar space (Reference 4). On the other hand, galactic electrons may be the decay products of pions produced by collisions of cosmic rays with interstellar matter (Reference 5). The possibility of identifying the major source of galactic electron production could yield information regarding the origin of cosmic radiation, the injection and acceleration mechanisms involved, and the medium through which they reach the earth's vicinity. Similar arguments may be presented regarding the electronic component in solar cosmic rays which again has been found (Reference 6) to be very small—the absolute upper limit on electrons/protons above 450 Mev/c was set at about 1 percent. Thus it is apparent that the scarcity of high energy primary electrons and the difficulty in attempting to separate them from the secondaries in the low-energy region imply that their study will be as difficult as it is important.

The origin of low energy electrons ($E < 100$ Mev) at balloon altitudes and at high geomagnetic latitudes cannot be established easily because it reflects the uncertainty characteristic of the calculated geomagnetic cutoffs for these latitudes. However, considerable information may be obtained by discriminating between positively and negatively charged electrons. In a shower, equal numbers of relativistic positrons and negative electrons are produced. Electrons produced in processes such as ionization, beta decay and the decay of mesons from nuclear interactions, will have different positive-to-negative charge ratios. With regard to electrons produced in the earth's atmosphere by cascade processes (whether they originate in the atmosphere above the detector or in the opposite hemisphere) we can expect to find equal contributions from particles of opposite charges. If, however, an appreciable number of the electrons detected represents a primary flux, in which the positron-to-electron ratio is not identical with that characteristic of shower products, we may attempt to investigate this flux by the charge unbalance that it will produce at balloon altitudes. Thus, in principle, it might be possible to obtain clues with regard to the origin of solar and galactic electrons. If they are basically negatively charged, they would indicate an injection process which is not of a nuclear character. But, on the other hand, since most of the secondary galactic electrons which are produced in nuclear interactions are due to proton-proton collisions, a considerable amount of a positive excess can be expected in the low-energy region of the galactic electronic component, if such collisions represent the dominant source. The amount of this excess has been calculated as a function of energy (Reference 5). It is more pronounced at energies below 100 Mev.

To measure the positron-to-electron ratio, a detector must accomplish two things. It must first identify an incoming particle as an electron, then determine the sign of its charge. We may do this using a cloud or a spark chamber with a magnetic field arrangement. However, if the investigation is confined to electrons with energies not exceeding a few tens of Mev, a simpler way would be to stop these particles inside an absorber with a large radiation length and a low photoelectron conversion efficiency (such as plastic scintillator), and then detect one or both of the annihilation quanta from stopping positrons as shown in the simplified diagram of Figure 1. A detector is described whose operation is based along this principle. Design and construction problems, calibration techniques, etc., will be discussed in detail. By using actual balloon flight data to demonstrate the feasibility of this detecting technique, some of its limitations will become obvious.

PRINCIPLE OF OPERATION

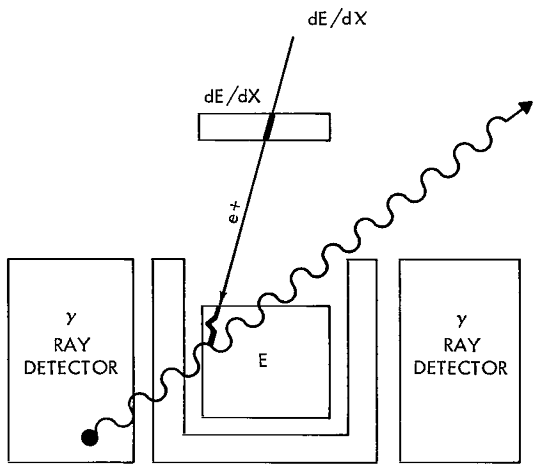

Figure 1—Simplified diagram indicating the detection of a positron.

The different functions of the detector are performed by scintillator-photomultiplier combinations. The effectiveness of this detector depends greatly upon the proper choice of scintillating materials for each function. To see this, consider a rather simple description of the mechanism on which the design of the detector is based. Here the aim is to stop an electron inside a scintillating material, then to utilize the presence or absence of annihilation photons to determine the sign of the charge. Obviously, the latter function can be meaningful only if the probability of a positron being created inside the stopping material through a radiation-pair production sequence is negligible, for electrons with energies of the order of the energy of a deep-penetrating stopping electron. An electron passing through matter, loses energy partly by ionization and partly by radiation.

The ratio of the radiation-to-ionization rate of energy loss for relativistic electrons is approximately proportional to the atomic number of the absorbing material for a given incident particle energy (Reference 7). In view of the importance of minimizing radiation losses, we must therefore select a scintillator with low atomic number. It must be added that in so doing, we also minimize the probability of a pair-production process since, for a given electron and photon energy, radiation phenomena and pair production show similar dependences on the atomic number of the material (Reference 8). The use of a low-atomic-number material is also demanded by the following argument. The γ rays from positrons annihilated inside the stopping scintillator must traverse a thickness of this material of the order of one of its dimensions before being detected. It is imperative that the average energy loss in this traversal be very small when compared to the energy of the γ ray if the positron detection efficiency is not to suffer. The mean free path of a γ ray decreases as the atomic number of the material being traversed increases.

All these arguments strongly suggest that a light material such as a plastic scintillator should be by far more suitable as an energy absorber than materials such as NaI or CsI. It is of interest to note that plastic scintillating materials have a nearly linear pulse-height response as a function of electron energy which simplifies the task of energy calibration (Reference 9). Now we shall investigate the proper choice of scintillating material for the detection of the 0.511 Mev photons which are coincident with the stopping positron.

Of the three dominant γ ray interactions with matter, pair production is obviously not of interest in this case. The Compton effect, as indicated by the corresponding mass-absorption coefficient, is nearly independent of the atomic number of the material, whereas the photoelectric effect becomes increasingly important as the atomic number increases. A Compton interaction results in partial absorption of the photon as compared to total absorption when a photoelectron is produced. Obviously, any number of successive Compton interactions followed by a photoelectron will also result in total photon absorption. Total absorption is essential if good discrimination is to be achieved through the use of a narrow energy window. Good discrimination is highly desirable since, in order to achieve realistic positron detection efficiencies, massive γ ray detectors must be employed, with the result that high counting rates are to be expected. Furthermore, the contribution of coherent effects such as knock-on electrons, showers, bremsstrahlung, etc., will be minimized. The probability of total γ ray absorption will be increased when a scintillator with a large atomic number such as CsI is used. Even in this rather heavy material, the mean free path of a 0.511 Mev photon is about 4 cm, so that reasonably large efficiencies will be obtained only after using quite large crystals, closely surrounding the stopping scintillator.

We have not yet established a method by which a particle can be identified. A charged particle is uniquely identified (except for the sign of its charge) by its total energy and the rate at which it loses energy when it traverses a given material (Reference 10). The latter can be determined from the light produced when the particle in question passes through a thin scintillator before entering the energy absorber. For good resolution, this absorber should be as thin as is consistent with a reasonable light output. If the particle subsequently enters and stops in the large scintillator, the total energy can be measured in a similar way. Obviously, it is absolutely essential to know whether the particle re-emerged from this scintillator after entering it, as the energy loss indicated by its light output would then represent only a partial energy loss. Such partial losses may be determined by placing a guard counter, in the form of a cup around the energy measuring scintillator. Electrons, in contrast to other particles, are particularly easy to identify because they are relativistic (and therefore produce essentially constant ionization in matter) down to energies of a few kev. To determine the type of scintillating material which we must use for the construction of the guard and thin (dE/dx) scintillators, we can follow the same sort of reasoning which we used in selecting the material for the energy absorber. The same requirements, namely low radiation losses and good transparency to the 0.511 Mev photon point to plastic scintillator as the material best suited for these detectors.

DESIGN AND CONSTRUCTION

A simplified layout of the detector is shown in Figure 2. Altogether, there are seven scintillators, four of which are the massive γ ray detectors forming a cylindrical shell around the energy scintillator guard-counter combination. All scintillators are optically isolated from each other and are therefore viewed by separate photomultipliers. The PM tubes corresponding to the thin (dE/dx) scintillator and the energy (E) absorber are the only ones not in optical contact with their respective scintillators. In the case of the dE/dx scintillator this is probably advantageous since, with this arrangement, the usual photocathode nonuniformities will not present any major problem.

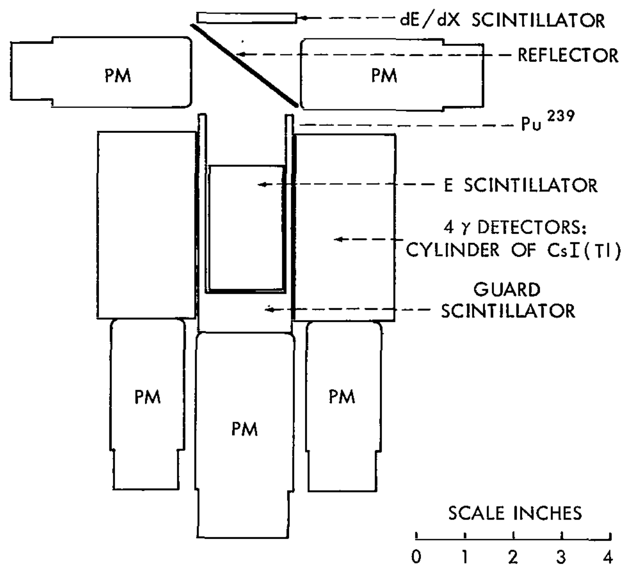

Figure 2—Simplified layout of the positron detector.

In choosing a plastic scintillator as the material for the energy absorber on the basis of the aforementioned considerations, we may easily see that the energy range of the detector will now depend solely upon the size of this scintillator. We have seen that the annihilation of a positron inside the E scintillator will for all practical purposes result in two photons emitted in opposite directions. If we now introduce the reasonable requirement that for every such annihilation there is always a direction of emission for which both photons may be detected simultaneously by any pair of CsI crystals, we see that the size of the energy absorber will be limited by that of the γ ray detectors. The design of this scintillator must also be consistent with a diameter-to-length ratio that will not introduce major light collection problems, especially from energy losses at the lower portions of this cylindrical absorber. In practice, the size of the CsI counters is limited by factors such as availability, cost, and weight. The dimensions of the CsI quadrants used in the construction of this detector, along with the dimensions of the E scintillator, may be seen in Figure 2.

Measurable 2γ detection probabilities can be expected for positrons of minimum and maximum penetrations, since the energy absorber was made somewhat smaller than the CsI quadrants. With this arrangement, the average energy dissipated inside the absorber by a minimum ionizing particle penetrating its entire length, is about 15 Mev. Some higher energy electrons will stop inside the E scintillator, partly due to scattering and partly to radiation losses. The latter are expected to be quite small for electrons in this energy range (Reference 11).

The dE/dx counter was also made of plastic scintillator material about 0.4 gm/cm^2 (700 kev) thick. This was found to be a satisfactory thickness for adequate light collection with the proper choice of a reflecting paint. The same thickness was chosen for the cylindridal shell of the plastic scintillator surrounding the E counter as shown in Figure 2. It is clear that the importance of this guard counter cannot be over-emphasized. At first, it may be thought that its efficiency is marginal since most of the cup is considerably removed from the photocathode of the PM tube. However, as will be seen, adequate measures were taken to insure a high efficiency. The latter is largely due to the fact that the thin, well-polished shell is an efficient light pipe for the light output of particles crossing the upper portions of the cup. That is, light is transmitted by multiple internal reflections at the walls of the shell. It is important that the photomultiplier be optically coupled to the entire bottom surface of this scintillator, so as to provide a more direct path to the photocathode. For this reason, a 2-inch tube is used with this counter.

The design of the housing for this detector must be carefully considered, since some difficulties arise with regard to packaging the large and heavy CsI crystals. The housing material must be kept to a minimum to reduce background problems. At the same time the detector must be made sufficiently sturdy and the quadrants must be tightly packaged as even small shifting will damage the coated walls of the housing and alter the optical coupling at the crystal-photomultiplier interface. The optical isolation of each quadrant is also somewhat difficult because the latter must be accessible and removable in the event that a change is necessitated. The detector housing is shown in Figure 3.

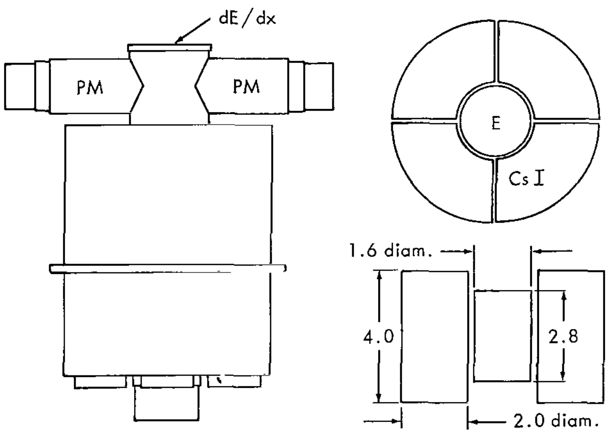

Figure 3—The housing of the positron detector.

The proper use of reflecting materials is of particular importance in this case, since in most instances we have been forced to use a geometry which is not very conducive to efficient and uniform light collection. It appears that for a given reflecting material such as an oxide, the effectiveness of the paint is greatly dependent on the binding substance that is being used. The best results were obtained with an experimental TiO_2 paint whose binder composition is not known. Coatings obtained by spraying this paint were adequate in many cases but they were rather brittle. When greater strength was necessary, a mixture of TiO_2 powder with clear epoxy was found to be satisfactory. Such a mixture was used to paint the walls of the CsI crystal housing, as chipping would have been unavoidable here with a brittle coating. This paint can also be applied directly on plastic scintillator, where it forms a durable bond provided that the surfaces have been made rough and have been thoroughly cleaned. Both the energy and the rate-of-energy-loss scintillators were thus coated on all their faces except the one facing the corresponding PM tube. No coating was applied on the guard scintillator since total internal reflection was relied upon in this case for light transmission. Neither was this paint applied on the CsI crystals, because the long term effects of the epoxy resin on this material are not adequately known. However, it may be mentioned that, had these large scintillators been painted, their packaging problems would have been considerably simplified.

Figure 4 shows the block diagram of the electronic instrumentation which accompanies this detector during a flight. It may be briefly described as follows: Whenever pulses above a given threshold occur in coincidence in the E and dE/dx scintillators, an electronic gate is created which gates the pulses from these scintillators into two 32-channel analyzers. The two five-bit digitized outputs, as well as five additional bits corresponding to the gated outputs of the four γ-ray detectors and of the guard counter are stored on magnetic tape. An additional bit is used to indicate the occurrence of an event, as both the E and the dE/dx outputs include an overload feature in which energy losses greater than a certain upper energy limit are indicated by the absence of all bits

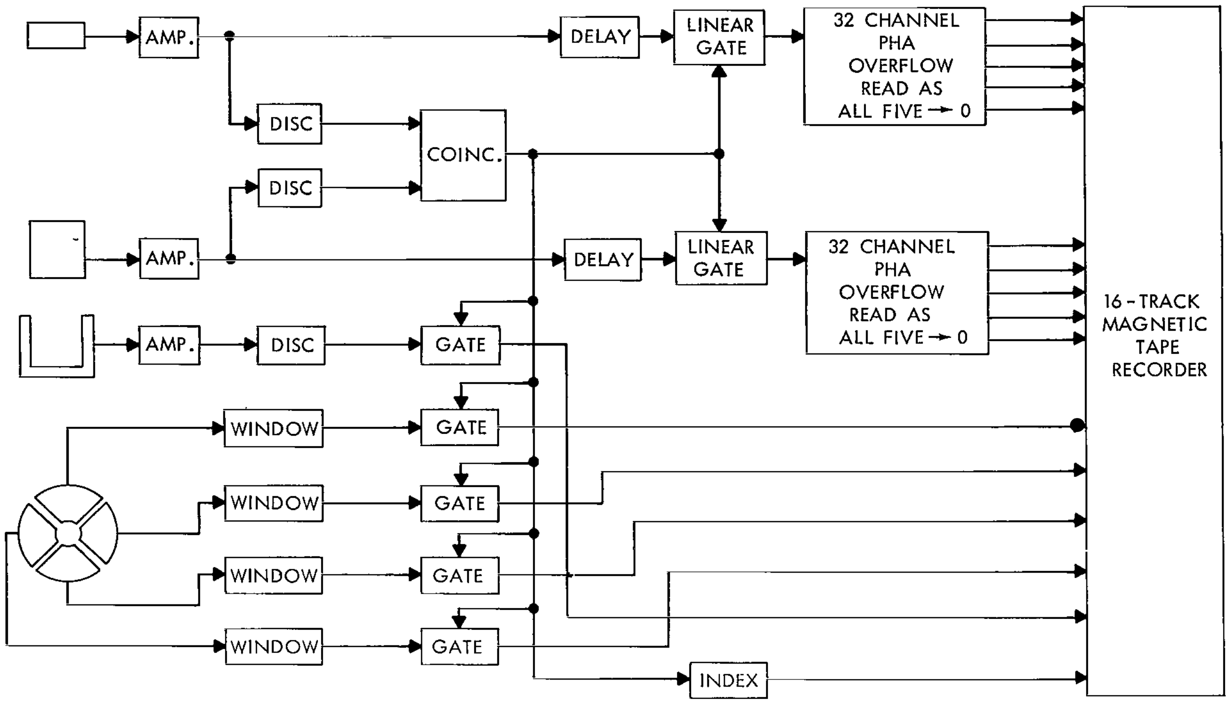

Figure 4—Block diagram of the electronic instrumentation.

in the corresponding output. The memory of the apparatus consists of a 16-track tape recorder, capable of continuous operation for a duration of about 14 hrs, using 3/4-inch magnetic tape at a rate of approximately 10 in/min. It has been found that the recorded data can be recovered properly as long as the separation between successive events is greater than about 0.1 mm. To insure that this is indeed the case, following each event the electronics are deactivated for a period sufficiently long for the tape to advance the minimum distance necessary. It is easily seen that the tape speed puts an upper limit on the number of events that may be processed in a given time interval. From flights already conducted during quiet times it was found that the pulse-rate capabilities of the system as described, are adequate for periods of low solar activity. For example, the normal counting rate at Churchill, Canada was found to be about 4 counts/sec. However, as the available margin extends only by about one order of magnitude over this normal pulse rate, it is expected that the present equipment will provide only partial information during a period with a marked increase in solar activity.

The analog-to-digital converters are commercially available units and operate on the usual principle of gating an oscillator of a given frequency by a time base which is proportional to the pulse height of the event to be analyzed. An energy window was used in the output of each γ ray detector to reduce the random coincidence rate. The circuit is shown in Figure 5. The width of this window was adjusted at about 500 kev. This range was found to be adequate to account for the resolution of the 0.511 Mev line in each detector (about 200 kev) and for expected small signal drifts due to temperature and/or voltage fluctuations and to small changes in the interface coupling between the PM tube and corresponding crystal.

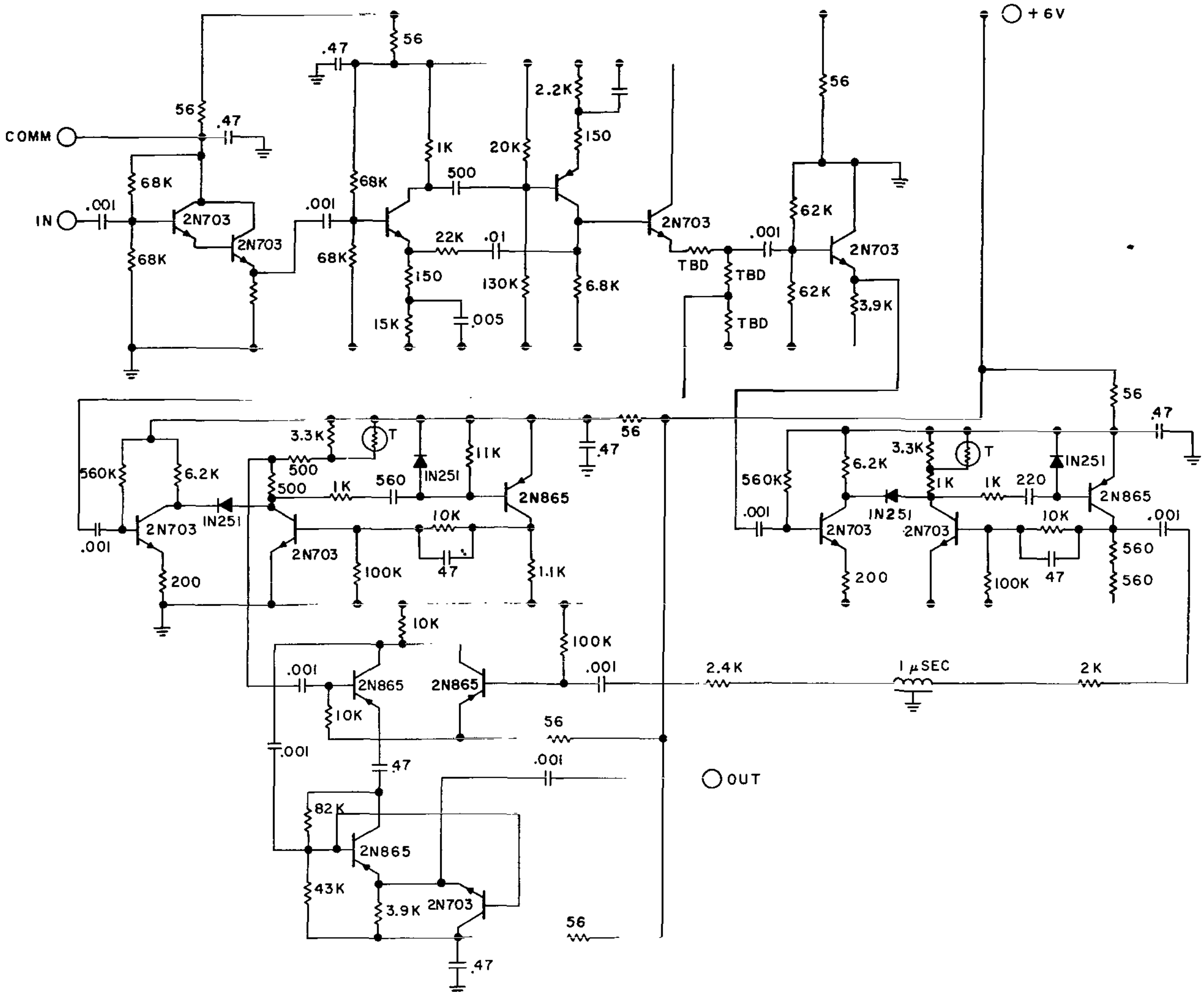

Figure 5—Energy window circuit.

LABORATORY CALIBRATION

Radioactive sources and the sea-level component of cosmic radiation were utilized in the laboratory calibration of the detector. The sea-level secondaries, although very infrequent, are invaluable in such a calibration, as they represent the most readily available source of penetrating particles. It is obvious, however, that statistically meaningful information can only be obtained after long periods of operation. This may be done either by using the apparatus with its own analyzers and data storage or by employing an external pulse-height analyzer, appropriately gated by a dE/dx and E coincidence. The latter method is usually more convenient for it does not present the data reduction problems which the former presents. As practically all of the sea-level secondaries which produce a coincidence are relativistic, we obtain from the dE/dx scintillator output a pulse-height distribution characteristic of minimum-ionizing particles. In view of the fact that we are describing an electron detector, this distribution and its position in relation to the 32 channels of the corresponding analyzer are of primary importance. Figure 6 shows a distribution obtained using an auxiliary multichannel analyzer. The energy losses of the penetrating particles in the energy absorber (with anticoincidence count required) will cover the energy range from the threshold of the coincidence circuit to the energy lost by a particle traversing the entire length of this scintillator. In Appendix A it is shown that the energy distribution should be peaked at the average energy corresponding to such a maximum traversal. The position of this peak relative to the pulse-height analyzer range is again of primary importance. It should finally be mentioned that these fast secondaries provide a very important check on the efficiency of the guard counter. The overwhelming prevalence of relativistic particles means that nearly every coincidence should be accompanied by an anticoincidence pulse.

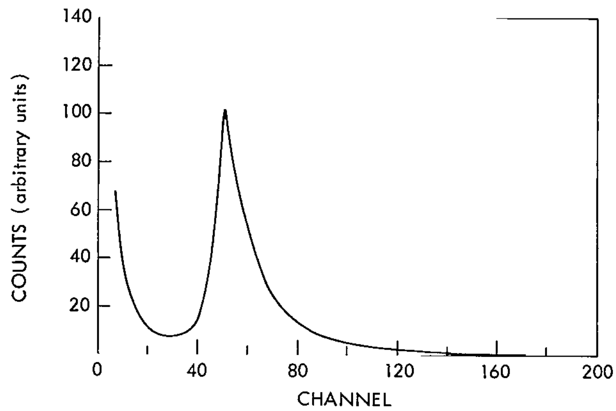

Figure 6—The dE/dx pulse-height distribution of sea-level μ mesons.

Such "μ-meson runs" constitute the major part of the final calibration just prior to a flight, at a time when the balloon apparatus operates entirely as a self-contained unit.

Radioactive sources are essential in this type of work. In fact, most of the preliminary tests, as well as certain preflight calibrations, are accomplished through their use. Source calibration is obviously much quicker. A description of the various sources used and of the information obtained is as follows:

A Cs^{137} source (660 kev photons) was used with the dE/dx and E scintillators and with the CsI quadrants in determining the best housing arrangements, best reflecting paints and method of application for best resolution. In a plastic scintillator, the criterion which may be used as a measure of its resolution is the shape of the experimental spectrum of the recoil electrons from Compton collisions. Under the best experimental conditions, the predicted sharp peak (Reference 12) at the cutoff energy in the electron energy distribution of Compton electrons, is barely seen. However, a good qualitative resolution criterion may be adopted from the shape of the resulting plateau in the distribution. In the CsI scintillators, where the dominating interaction is the photoelectric effect, the width and the peak-to-valley ratio of the resulting photopeak can be used as resolution criteria. The pulse-height distributions of the 660 ev photons from Cs^{137} in plastic and CsI are shown in Figure 7. A Na^{22} source (positron emitter) is used to produce the 0.511-Mev peak in the γ ray detectors. This peak is in turn used to adjust the energy window at the output of each detector. This adjustment is part of the preflight calibration.

Finally, a Pu^{239} α source is permanently placed on the thin portion of the guard counter, (see Figure 8) about 1/4 inch from its most remote section from the PM tube. The apparent energy

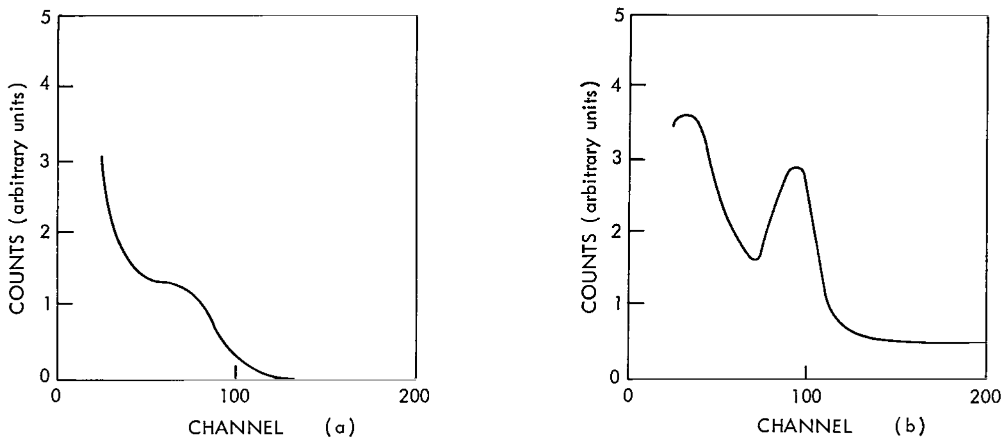

Figure 7—Pulse-height distribution of 660 kev photons in: a, Plastic scintillator; b, CsI scintillator.

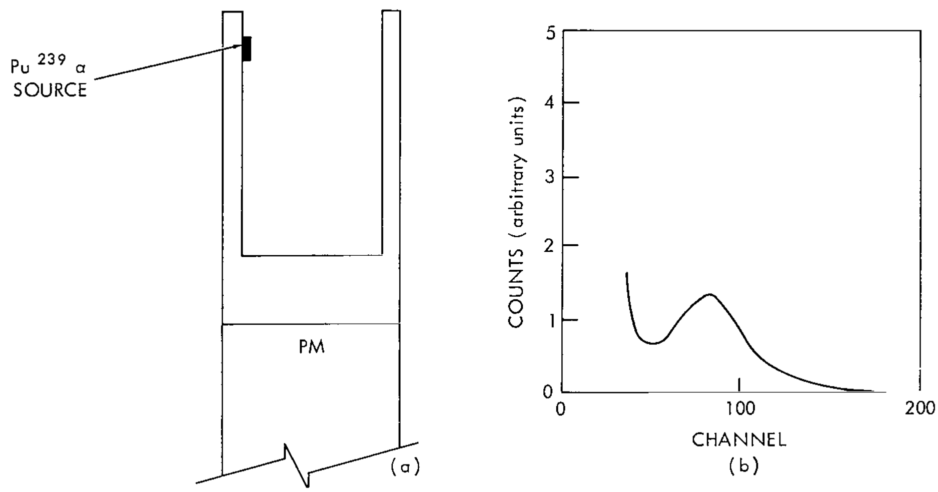

Figure 8—Calibration of the guard scintillator: a, Position of the source; b, Pulse-height distribution.

loss of these α particles in the plastic scintillator (when compared to energy losses of electrons) is about 250 kev whereas the most probable energy loss of a minimum ionizing particle through the thinnest portion of this counter is about 700 kev. The threshold of this detector is adjusted to pass the entire distinct spectrum of the α particles. This spectrum, shown in Figure 8, is indicative of the good resolution attained even for energy losses at large distances from the PM tube. The better than 3:1 minimum safety factor is considered adequate. In the absence of a pulse-height analyzer, pre-flight calibration consists of the requirement that the counting rate of this detector does not drop below a predetermined minimum rate of about 40 counts/sec.

We may note that no attempt was made to develop a laboratory technique for determining the positron detection efficiency of this detector as a function of energy. Instead, it was planned to calibrate the latter using ascent data from the vicinity of the Pfotzer maximum. At such atmospheric depths, it is reasonable to assume that the positron-to-electron ratio in the energy interval of interest approaches the value of one.

FLIGHT DATA AND DISCUSSION

Some flight data will now be presented and briefly discussed. The flight took place over Fort Churchill, Manitoba, Canada, on July 16, 1962 and reached a ceiling altitude of approximately 4 gm/cm^2 (126,000 ft.). Figure 9 shows a plot of the dE/dx versus E pulse heights, for particles stopping in the E scintillator. The minimum ionizing region is quite distinct. It may be noted that the energy losses due to protons lie completely outside this region, i.e., an overload pulse in at least one of the analyzers is expected when a proton is detected. In Figure 10 the dE/dx distribution of stopping particles is compared with that of penetrating particles. The two distributions are quite similar in the minimum ionizing region, as we might expect, since a high percentage of the penetrating particles is relativistic. The characteristic asymmetry due to statistical fluctuations in the energy loss in a thin absorber (Reference 13) is quite discernible. Similar distributions for the energy loss in the E scintillator, for the same two groups of particles, are shown in Figure 11. Only particles whose dE/dx loss indicated minimum ionization were included. The peak in the penetrating particle distribution corresponds to the average energy loss by a relativistic particle penetrating the entire length of the detector. The location of this peak during the duration of the flight may be traced back and appropriate corrections may be made in case of substantial drifting. The correspondence between this peak and the less conspicuous, discontinuous decline in the number of electrons in this energy region is clear. The differential and integral energy distributions for the electronic component at about 4 gm/cm^2 are shown in Figure 12. Note that these are not energy spectra as the geometric factor of the detector has not been taken into account. With regard to this factor, it is easily seen that its value depends on energy or equivalently on the penetration in the E scintillator. At low energies, it is poorly defined due to the large scattering angles

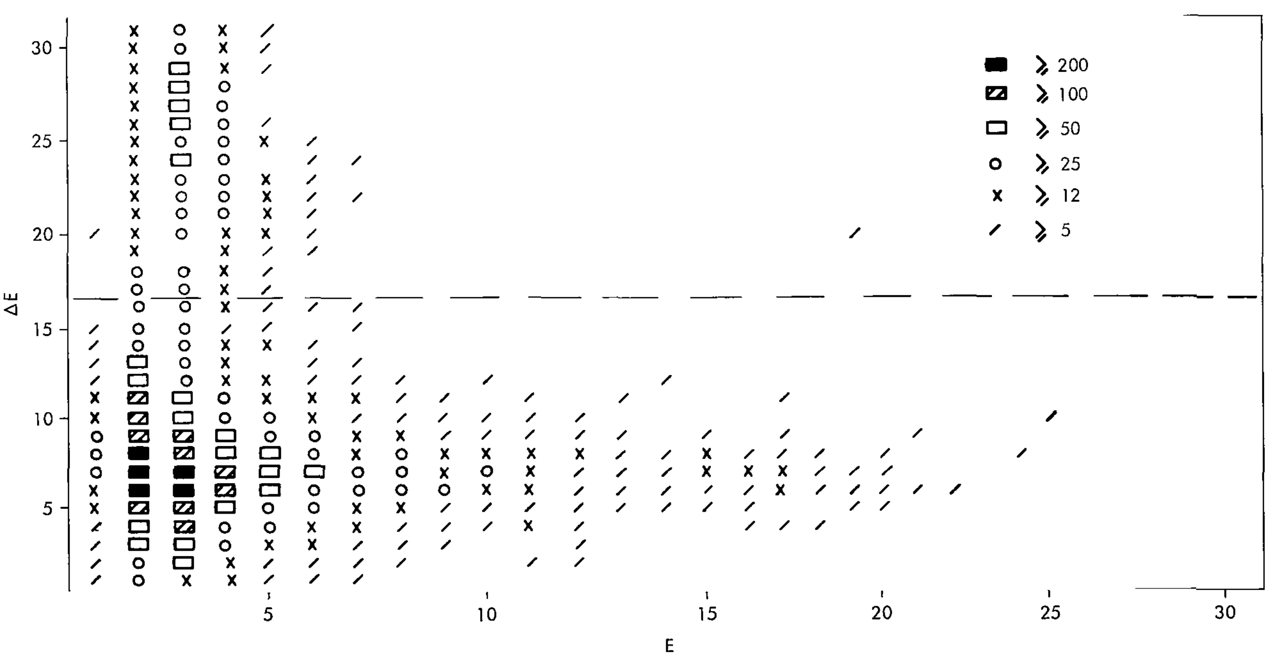

Figure 9—dE/dx versus E plot of stopping particles.

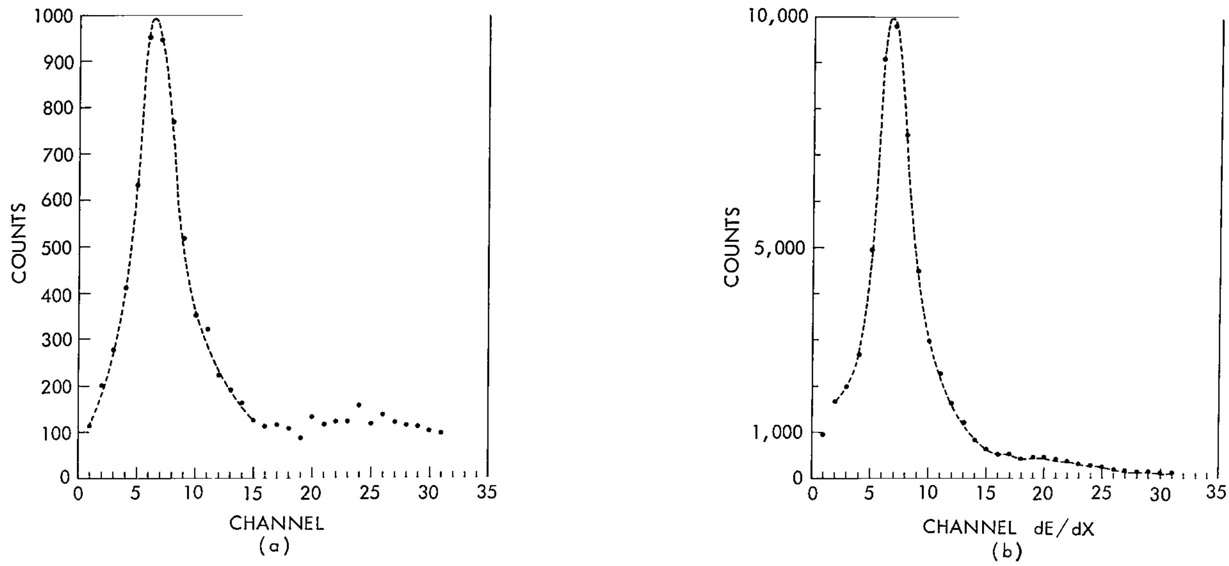

Figure 10—dE/dx pulse-height distributions: a, Particles stopping in E; b, Particles piercing E.

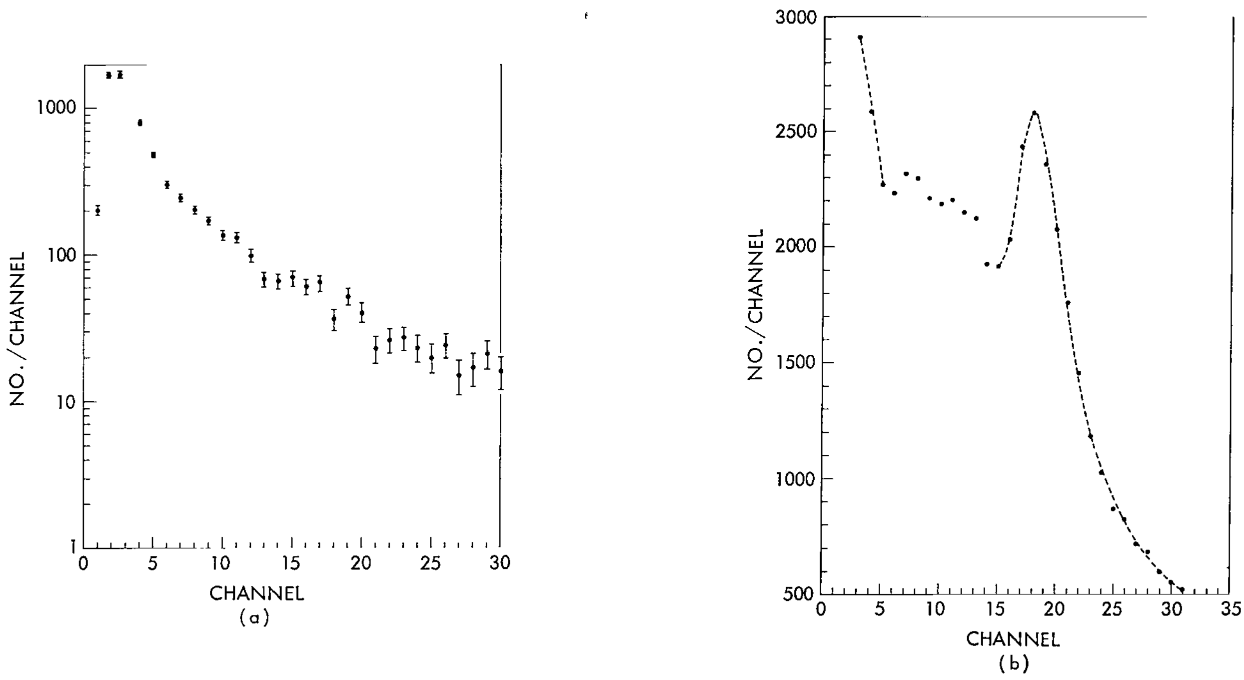

Figure 11—E pulse-height distributions: a, Particles stopping in E; b, Particles piercing E.

of low energy electrons. However, it will be of some interest to note that on the basis of purely geometrical considerations, approximate calculations yield a geometric factor which varies from about 4 to 1.2 corresponding to the lowest and to the highest energies that may be detected. The relative electron abundancies in the three groups characterized by: (1) no coincident photons;

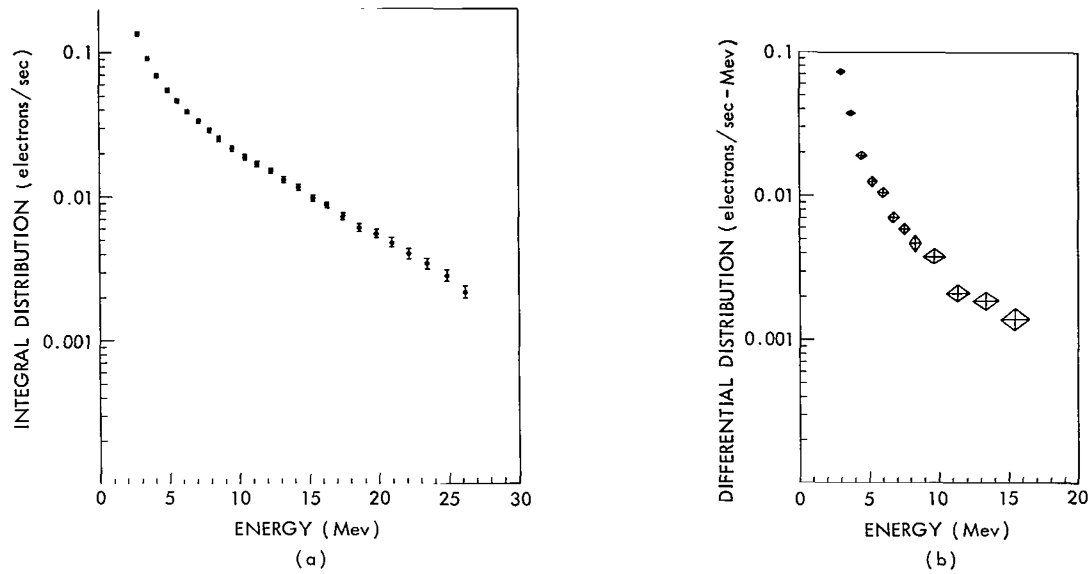

Figure 12—Electron energy distributions: a, Integral; b, Differential.

(2) one coincident photon; and (3) two coincident photons are shown on Table 1. The relatively small number of 2-γ events reflects a low positron detection efficiency rather than a large electron excess at the top of the atmosphere. Considering the fact that the data shown represent an approximately 10-hour collection period and that with the present arrangement similar data will be required from the region near the Pfotzer maximum (which the balloon traverses in a matter of 20 minutes or so) before any conclusions concerning the energy dependence of the positron-to-electron ratio at ceiling can be made, it becomes obvious that no statistically significant information about this ratio can be expected from the two-γ events alone. The one-γ events are statistically more promising due to a considerable increase in efficiency. Here, however, other difficulties become more pronounced, of which the most serious is an increase in the number of coincidences not associated with positron annihilation, whether purely random (see Appendix B) in character or related in some manner with the particle being detected (i.e., showers, knock-on electrons, bremsstrahlung, etc.). It is probably best to rely entirely on the two-γ events by conducting an accurate laboratory calibration of the detector in order to obtain its positron detection efficiency as a function of energy. Even so, it is doubtful whether small changes in the positron-to-electron ratio (for example less than 20 percent) can be clearly established from a typical balloon flight. The situation may of course change entirely in the case of solar events when substantially larger counting rates may be encountered.

Table 1

Number of Electrons in Each of 5 Channel Groups.

Number of Electrons	Channels				
	1-4	5-8	9-12	13-16	17-31
With no γ rays	3494	965	387	203	325
With 1 γ ray	625	215	120	41	69
With 2 or more γ rays	138	53	24	19	17

We may attempt to establish an integral electron intensity from the data presented here by using the approximate geometric factors mentioned above. Such an intensity probably represents a lower limit since electron scattering into the guard counter will tend to remove many electrons whose assumed straight-line trajectories would group them among those stopping inside the E scintillator. We thus arrive at about 0.03 electrons/cm^2-sec-ster for electrons with energies greater than 3 Mev at 4 grams/cm^2. This number compares favorably with the intensity of approximately 0.04 particles/cm^2-sec-ster for electrons of comparable energy measured by Meyer and Vogt (Reference 1) at about the same location and altitude in the atmosphere.

CONCLUDING REMARKS AND WAYS OF IMPROVEMENT

A detector has been described which, from all indications, can provide considerable information on electrons from about 1 to 15 Mev, at atmospheric depths which can be attained by balloon-borne equipment. The detector was primarily designed to measure the positron-to-electron ratio as a function of energy at different atmospheric depths. It has become apparent, however, from existing data, that due to the low detection efficiency for annihilation photons, data collection times at any particular atmospheric depth of interest must at least be of the order of several hours before sufficient statistical accuracy can be achieved to warrant any conclusions. In view of the fact that in a typical flight the balloon achieves ceiling altitude about two hours after launch, it is clear that we cannot expect to obtain any significant ascent data unless special provisions are made for a step flight. Specifically, it seems that a laboratory calibration of a positron detection efficiency of the detector will be necessary for the proper interpretation of ceiling data instead of the previously stated intention to obtain such a calibration from data in the vicinity of the Pfotzer maximum. In general, it is doubtful whether this detector, however improved, will be instrumental in detecting a small (i.e., less than 20 percent) positive or negative electron excess (if such an excess exists) at the top of the atmosphere, with the possible exception of periods of increased intensities resulting from solar activity. However, a version suitable for satellite use may very well be flown on a satellite where more adequate and useful data is anticipated.

There are several areas in which improvements and additional work would be desirable. One of these, the need for a thorough calibration of the detector efficiency, has already been mentioned. Difficulties have been experienced in maintaining the optical coupling between the heavy CsI crystals and the corresponding PM tubes. Silicone grease was probably a poor choice in this case. A better performance can probably be achieved through the use of materials such as some commercial gels which upon curing maintain their form as well as their adhering properties indefinitely.

It will be desirable to reduce the number of false positron coincidences. We may do this either by decreasing the width of the energy window at the output of each γ ray detector or by increasing the resolution of the corresponding coincidence circuits, or both. The former attempt would necessitate better stability throughout (low and high voltage power supplies, optical coupling, temperature drifts, etc.) while the second would simply involve the use of faster coincidence circuits. It is estimated that the number of false counts in each crystal can be reduced by about a factor of 10, in which case greater faith can be placed on the more numerous one-γ coincidences.

It appears that it would be advantageous to have a record during the flight of the counting rate of one of the window outputs so that part of the uncertainty in our estimate of false γ ray counts may be eliminated. Furthermore, it may even be interesting to consider replacing the 32-channel analyzer which processes the dE/dx energy loss with an energy window and use the analyzer to process the outputs of the CsI crystals.

Finally, it is believed, in view of the importance of the guard counter, that the safety factor should be improved by increasing the thickness of the walls of the plastic scintillator cup. This may then allow the removal of the optical coupling, which is obviously desirable whenever possible.

ACKNOWLEDGMENTS

The author offers his sincere thanks to Dr. F. B. McDonald for his efforts in making this work possible as well as for his greatly valued advise and comments. And, further, he wishes to acknowledge numerous contributions by Dr. T. L. Cline who suggested this research and actively participated in the development of the apparatus and the analysis and discussion of data. Thanks are also extended to Professor J. B. Marion who supervised this thesis and to Drs. V. K. Balasubrahmanyan and D. Bryant for interesting discussions and valuable comments.

REFERENCES

1. Meyer, P., and Vogt, R., "Electrons in the Primary Cosmic Radiation," *Phys. Rev. Letters*, 6(4):193-196, February 15, 1961.

2. Critchfield, C. L., Ney, E. P., and Oleksa, S., "Soft Radiation at Balloon Altitudes," *Phys. Rev.* 85:461-467, February 1, 1952.

3. Earl, J. A., "Cloud-Chamber Observations of Primary Cosmic-Ray Electrons," *Phys. Rev. Letters*, 6(3):125-128, February 1, 1961.

4. Ginzburg, V. L., "The Origin of Cosmic Radiation," in: *Progress in Elementary Particle and Cosmic Ray Physics*, Vol. 4 (J. G. Wilson and S. A. Wouthuysen, eds.):337-421, Amsterdam: North-Holland, 1958.

5. Hayakawa, S., and Okuda, H., "Electronic Components in Galactic Cosmic Rays," *Progr. Theoret. Phys.* 28(3):517-528, September 1962.

6. Earl, J. A., "Cloud-Chamber Observations of Solar Cosmic Rays over Minneapolis on September 4, 1960," Minneapolis: Minnesota Univ. School of Physics, CR-45, June 1962; *also J. Geophys. Res.* 67(6):2107-2117, June 1962.

7. Evans, R. D., "The Atomic Nucleus," New York: McGraw-Hill, 1955, p. 609.

8. Rossi, R., "High Energy Particles," Englewood Cliffs, Prentice-Hall, 1952, p. 79.

9. Hopkins, J. I., "Electron Energy Studies with the Anthracene Scintillation Counter," *Rev. Sci. Instrum.* 22:29-33, January 1951.

10. Bryant, D. A., Ludwig, G. H., and McDonald, F. B., "A Scintillation Counter Telescope for Charge and Mass Identification of Primary Cosmic Rays," *IRE Trans. Nuclear Sci.* NS-9(3): 376-380, June 1962.

11. Cramer, J. G., Jr., Farmer, B. J., and Class, C. M., "A Scintillation Spectrometer for High Energy Beta Decays," *Nuclear Instrum. Methods* 16(3):289-300, August 1962.

12. Evans, R. D., "The Atomic Nucleus," New York: McGraw-Hill, 1955, p. 693.

13. Rossi, B., "High Energy Particles," Englewood Cliffs: Prentice-Hall, 1952, p. 34.

Appendix A

Calculated Path Length Distribution of Penetrating Particles

We will attempt here to show that simply from geometrical considerations we may expect a distribution for the energy loss in the E scintillator by penetrating particles which is of the same general form as that of the observed distribution. We will assume an isotropic particle flux since the comparison will be made for ceiling data. We will further assume that the light collection from the E scintillator is independent of the depth of the energy loss. Finally, the corresponding analyzer will be assumed to be linear throughout its range. Under these assumptions, the portion of the particle trajectory inside the volume of the energy absorber will be proportional to the energy loss. The problem is essentially therefore to consider all possible particle paths through a given element of area of the dE/dx scintillator and determine the corresponding "energy loss" for each trajectory that intercepts the energy scintillator. The calculation will be completed by summing over the area in one quadrant of the dE/dx scintillator. No attempt will be made to obtain any integrals in closed form. It is easily seen that this would present quite a formidable job. A numerical approach is by far easier through the use of modern digital computers. With such an approach the problem is reduced to one in analytic geometry. A trajectory or line in space through the point $(x_1, y_1, 0)$ (see Figure A1) is completely determined by its direction cosines with respect to a Cartesian coordinate system. The points of intersection of this line with the cylinder (E scintillator) are found and the distance between a pair of such points is determined. The necessary relations which must be used in the ensuing FORTRAN program are summarized below. All symbols refer to Figure A1. The result of the calculation is plotted in Figure A2.

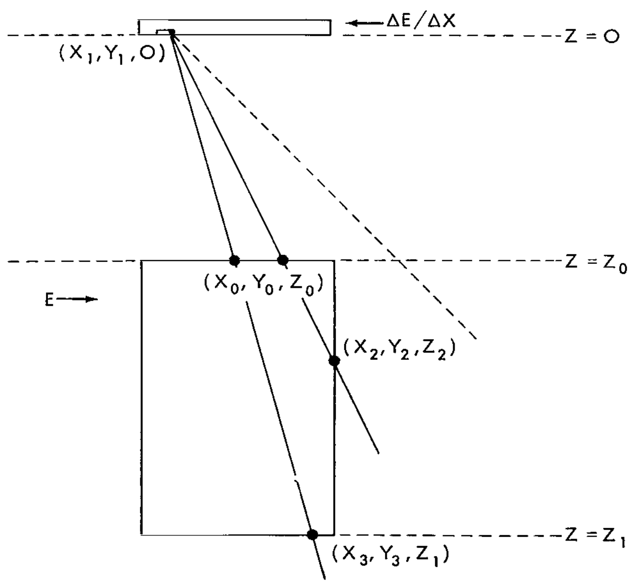

Figure A1—Geometric paths of particles piercing the E scintillator.

The distribution shown was obtained as follows: The calculated path-lengths were assorted into 18 groups, of which the last group contained the relatively large number of paths which cross the entire length of the detector. The number of paths in this last group was subsequently fitted to a gaussian distribution which was then superimposed on the remaining groups. The agreement between the experimental

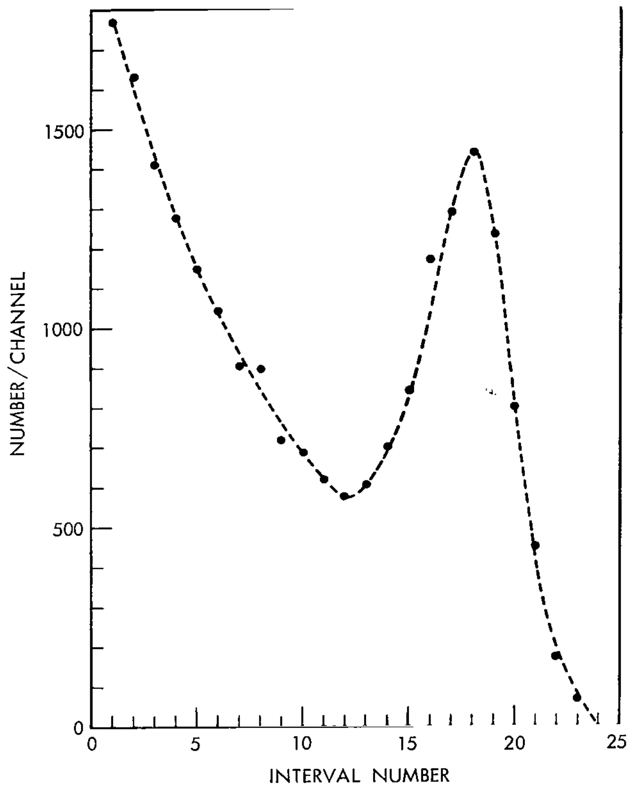

Figure A2—Calculated path distribution of particles piercing E.

(Figure 11, page 12) and calculated distributions is good. It is thought that the large background expected from the proximity of the massive CsI crystals is probably responsible for the filling of the channels before the peak where the largest disagreement occurs.

The following are necessary for the computation of the above distribution:

The equation of a line through the point $(x, y, 0)$ is

$$\frac{x - x_1}{\sin\theta\cos\phi} = \frac{y - y_1}{\sin\theta\sin\phi} = \frac{z}{\cos\theta} .$$

This line intercepts the $z = z_0$ plane at

$$x_0 = x_1 + z_0 \tan\theta\cos\phi$$

$$y_0 = y_1 + z_0 \tan\theta\sin\phi .$$

The condition for interception with the energy scintillator is

$$x_0^2 + y_0^2 \leq R_0^2 .$$

If the above condition is satisfied, then

$$z_2 = -\cot\theta\left(y_1\sin\phi + x_1\cos\phi\right) + \cot\theta\sqrt{\left(y_1\sin\phi + x_1\cos\phi\right)^2 - x_1^2 - y_1^2 + R_0^2} .$$

If $z_2 < z_3$, then $x_2 = x_1 + z_2\tan\theta\cos\phi$, $y_2 = y_1 + z_2\tan\theta\sin\phi$, and the path length is given by

$$L = \sqrt{\left(x_2 - x_0\right)^2 + \left(y_2 - y_0\right)^2 + \left(z_2 - z_0\right)^2} .$$

If $z_2 > z_3$, then $x_3 = x_1 + z_3\tan\theta\cos\phi$, $y_3 = y_1 + z_3\tan\theta\sin\phi$, and

$$L = \sqrt{\left(x_3 - x_0\right)^2 + \left(y_3 - y_0\right)^2 + \left(z_3 - z_0\right)^2} .$$

Appendix B

Estimated Random Coincidence Rate of γ Ray Detectors

An estimate will now be attempted of the random-coincidence rate of a γ ray detector at the balloon ceiling altitude using the corresponding electron intensity measured by the telescope. We may proceed in this manner to estimate the total number of "false positron" counts obtained at this atmospheric depth of 4 gm/cm^2 and compare this with the actual number of counts recorded during the flight.

Assuming that the measured intensity of .03 electrons/cm^2-sec-ster is isotropic we arrive at a flux of .38 electrons/cm^2-sec with energy greater than 3 Mev. The average thickness of the aluminum casing enclosing the CsI crystals was about .43 gm/cm^2, corresponding to an energy loss of about 1 Mev. The energy window at the output of each crystal will admit only electrons with energies roughly between 1.2 and 1.8 Mev to contribute to the total counting rate of each detector. Extrapolating the integral energy spectrum (Figure 12, page 13) we see that the above electron flux must be multiplied by at least a factor of 4 to become applicable to the above energy interval. Furthermore, since the energy spectrum is very steep in this energy region, we may simply use the approximate electron flux at the threshold of the window. We thus arrive at the following counting rate, due to electrons alone, for each γ ray detector which has an exposed area of about 202 cm^2:

$$R_{el} = 202 \times .38 \times 4 \approx 307 \text{ counts/sec} .$$

A contribution of the same order of magnitude may also be expected from γ rays. From published data* we see that a flux of roughly 0.8/cm^2-sec may be expected with energies in the interval covered by the window. Once again we see that the γ ray energy spectrum is very steep and since the probability of detection of a 200-300 kev photon by a CsI detector of the size used here is very high, we are justified in using the above flux in this calculation. We thus find that the γ ray contribution to the counting rate will be roughly

$$R = 202 \times 0.8 = 162 \text{ counts/sec} ;$$

*Peterson, L. E., "The 0.5-Mev Gamma-Ray and the Low-Energy Gamma-Ray Spectrum to 6 Grams per Square Centimeter over Minneapolis," *J. Geophys. Res.* 68(4):979-987, February 15, 1963.

and therefore that the combined contributions of both electrons and γ rays will be

$$R_{tot} = 469 \text{ counts/sec} .$$

The random coincidence rate for each detector is given by

$$R_{\tau} = 2\tau R_{tot} \times R_{tel} ,$$

where τ is the resolution of the coincidence circuit (here $\tau = 5\mu$ sec) and R_{tel} , the electron counting rate of the telescope, is in this case 0.186 counts/sec:

$$R_{\tau} = 2 \times 5 \times 10^{-6} \times 469 \times .186 = 8.7 \times 10^{-4} \text{ counts/sec} .$$

The total number of "false positrons" during a 10-hour flight will be about 125. From Table 1 of this paper we see that the number of positrons, as determined by the requirement of at least one coincident photon, during the same time interval, is 1321.

The above estimate of false counts does not include of course other components of radiation which contribute to the counting rate of a γ ray detector or coherent events whose contribution may be comparable or even greater than the number of random coincidences.

NASA-Langley, 1965

3118185
08

"The aeronautical and space activities of the United States shall be conducted so as to contribute . . . to the expansion of human knowledge of phenomena in the atmosphere and space. The Administration shall provide for the widest practicable and appropriate dissemination of information concerning its activities and the results thereof."

—NATIONAL AERONAUTICS AND SPACE ACT OF 1958

NASA SCIENTIFIC AND TECHNICAL PUBLICATIONS

TECHNICAL REPORTS: Scientific and technical information considered important, complete, and a lasting contribution to existing knowledge.

TECHNICAL NOTES: Information less broad in scope but nevertheless of importance as a contribution to existing knowledge.

TECHNICAL MEMORANDUMS: Information receiving limited distribution because of preliminary data, security classification, or other reasons.

CONTRACTOR REPORTS: Technical information generated in connection with a NASA contract or grant and released under NASA auspices.

TECHNICAL TRANSLATIONS: Information published in a foreign language considered to merit NASA distribution in English.

TECHNICAL REPRINTS: Information derived from NASA activities and initially published in the form of journal articles.

SPECIAL PUBLICATIONS: Information derived from or of value to NASA activities but not necessarily reporting the results of individual NASA-programmed scientific efforts. Publications include conference proceedings, monographs, data compilations, handbooks, sourcebooks, and special bibliographies.

Details on the availability of these publications may be obtained from:

SCIENTIFIC AND TECHNICAL INFORMATION DIVISION

NATIONAL AERONAUTICS AND SPACE ADMINISTRATION

Washington, D.C. 20546